Alonso, E., Gallo, A., Roldán, M. I., Pérez-Rábago, C. A., & Fuentealba, E. (2017). Use of rotary kilns for solar thermal applications: Review of developed studies and analysis of their potential. *In Solar Energy, 144*, 90–104

DOI:10.1016/j.solener.2017.01.004

Use of rotary kilns for solar thermal applications: review of developed studies and analysis of their potential

E. Alonso[a]*[¤], A. Gallo[a,b], M.I. Roldán[c], C.A. Pérez-Rábago[d] and E. Fuentealba[a]

[a] Universidad de Antofagasta. Centro de Desarrollo Energético Antofagasta, Chile. Avda. Angamos, 601, 1270300, Antofagasta, Chile.
[b] Doctorado en "Ciencias Aplicadas al Medio Ambiente" (RD99/11). Universidad de Almería, Spain.
[c] CIEMAT-Plataforma Solar de Almería. Ctra. Senés km 4 s/n, 04200, Tabernas, Spain
[d] Instituto de Energías Renovables. Universidad Nacional Autónoma de México. Avda. Xochicalco s/n, A.P. 34. Temixco, 62580 Morelos, Mexico.

*Corresponding author´s e-mail: elisa.alonso@uantof.cl
[¤]ISES Member

Abstract

Rotary kilns have a long history of use in classical industries. They are able to achieve high temperatures with higher thermal efficiencies than other reactor types. Their performance has been widely studied and classified according to different parameters. Since it is a well-known technology, rotary kilns have been selected for high temperature solar processes. This article initially presents a brief review of the rotary kiln technology and it focuses on the employment of these devices for thermal and thermochemical processes conducted by concentrating solar energy. Among the solar devices, a novel rotary kiln prototype for thermochemical processes is presented and compared with a static solar reactor. Finally, some practical conclusions on the design and operation of solar rotary kilns are remarked and an analysis of their main limitations is presented.

Keywords

Concentrating solar energy, rotary kiln, simulation, experimental

Nomenclature

Abbreviations

Al	Aluminium recycling
CaO	Lime production
CFD	Computational Fluid Dynamics
CIEMAT	Centro de Investigaciones Energéticas, Medioambientales y Tecnológicas

CNRS-PROMES	Centre National de la Recherche Scientifique - PROcédés, Matériaux et Énergie Solaire
CSP	Concentrating Solar Power
DLR	Deutschen Zentrumn für Luft-und Raumfahrt (German Aerospace Centre)
DO	Discrete Ordinates method
IER-UNAM	Instituto de Energías Renovables-Universidad Nacional Autónoma de México
MC	Monte Carlo ray tracing
PSA	Plataforma Solar de Almería
PSI	Paul Scherrer Institut
S2S	Surface-to-surface model
SD	Soil Decontamination
SPSR	Solid Particle Solar Receiver
TCS	Thermochemical Storage
TES	Thermal Energy Storage
WSTC	Water Splitting Thermochemical Cycle

Symbols

d	Inner diameter of the drum (m)
d_a	Diameter of the aperture (m)
F	Charge rate per unit of cross sectional area (kg s^{-1} m^{-2})
$FR\%$	Fill Ratio
Fr	Froude number
g	Gravitational acceleration (m/s^2)

h	Bed height (m)
$i.d.$	Inner diameter (m)
l	Length of the rotary kiln (m)
$\dot{m}_s$	Mass flow rate of the heat carrier solid
N	Rotational speed (rpm)
r	Inner radius of the drum (m)
s, v	Slope of the rotary kiln (°)
T_0	Temperature of cooling water
T_∞	Input temperature of air through the kiln entry
T_a	Output temperature of air through the kiln entry
T_b	Average temperature inside the rotary kiln
T_s	Output temperature of the heat carrier solid
$T_{s'}$	Input temperature of the heat carrier solid

Greek Symbols

τ	Residence time (s)
θ_d	Dynamic angle of repose (°)
ω	Rotational speed (rad/s)

1. Introduction

Currently, most of the commercial technologies based on concentrating solar energy are employed for the generation of electricity. These technologies consist in several square meters of mirrors for concentrating the solar radiation and can be also employed to produce high temperature heat for advanced applications. They include the production of solar fuels, such as hydrogen and synthesis gas, for the transportation sector and several industrial processes. The production of solar fuels is based on H_2O/CO_2 splitting (Abanades et al., 2006; Agrafiotis et al., 2015; Chueh et al., 2010; Francis et al., 2010; Fresno et al., 2009; Orfila et al., 2016; Roeb et al., 2011; Schunk et al., 2008, 2009) and decarbonisation

processes (cracking (Maag et al., 2009), reforming (Bianchini et al., 2015; Fuqiang et al., 2015) and gasification of carbonaceous feedstock (Piatkowski et al., 2009; Puig-Arnavat et al., 2013)). Among the industrial applications of concentrating solar heat, it can be remarkable the production of commodities like ceramic materials or metals. For example, some literature works are devoted to produce lime (Meier et al., 2004, 2005b, 2006) through the solar calcination of $CaCO_3$. The production of Zn from ZnO has been tackled through different solar reduction techniques, mainly carbothermal (Wieckert et al., 2004) and methanothermal reduction (Steinfeld et al., 1995), as well as the production of aluminium (Halmann et al., 2007). The solar recycling of aluminium has been also investigated (Glasmacher-Remberg et al., 2001). All the mentioned processes can be currently considered the most promising applications of concentrating solar heat . Also, since last few years, the concept of using concentrated solar heat as energy source for high temperature thermochemical reactions is being applied to store solar energy. Reversible reactions are employed to store energy during the endothermic step and release it during the exothermic one (Agrafiotis et al., 2014; Neises et al., 2012; Pardo et al., 2014).

The above indicated applications involve the heating of solid materials with solar radiation and this represents an important research challenge. Among the contributions to their development, studies on receiver/reactor design play a relevant role. The concepts based on the direct heating of solid particles are the more interesting. Solid particles are able to absorb radiation and storage the heat in the form of sensible and/or chemical energy. The absorption efficiency is improved when radiation and particles have direct contact –without any opaque barrier. A remarkable advance related with this idea took place in 1980's, with the development of the first concept of Solid Particles Solar Receiver (SPSR) (Kim et al., 2009). Particles, which acted as heat transfer medium, absorbed the radiation inside a cavity receiver. The heat was then transferred to a fluid, presumably steam or air. Apart from the absorption efficiency and the ease to storage the heat, the SPSR has remarkable advantages compared to central receivers that use different type of thermal fluid. For instance, using solid particles can be very economical, depending on the abundance of the selected material, and thermal stress can be reduced in plant components due to the direct absorption (Tan and Chen, 2010). Furthermore, particles can be heated to higher temperatures than other heat transfer media. Solar rotary kilns, which are the focus of this review, can be considered a particular type of SPSR (Alonso and Romero, 2015a). A first assessment has been recently presented, considering a rotary kiln filled with sand particles as central receiver of a 50 MW_{th} solar plant (Gallo et al., 2016). When these particle solar devices are aimed to perform chemical processes (for solar fuels or industrial applications, for example) instead of heating up particles acting as heat transfer medium, they can be called particles solar reactors instead of SPSR. Lots of solar particles reactors have been reported in literature with different configurations. Some authors have tried to innovate and to design novel engineering concepts (Diver et al., 2008; Kaneko et al., 2007). Many others have readapted classical technologies to integrate the direct solar radiation (Gokon et al., 2008; Meier et al., 2004; Nikulshina et al., 2009). Solar rotary kilns have been one of the most selected types of devices (Alonso and Romero, 2015a). The reasons are, probably, the advantages that the classical industry rotary kilns present in comparison with other classical gas-solid systems. Rotary kilns have a long history of use in metallurgical and chemical industries, their performance is well known and

they are able to operate at very high temperatures (over 2000 °C, although values of maximum temperature vary with the consulted source) with higher efficiencies than other types of devices. Additionally, they are versatile, they have low cost of maintenance and their components have long life.

The objective of this work is to analyse the potential of the rotary kilns when they are directly irradiated by concentrated solar energy. For that purpose, industrial rotary kiln features and applications have been firstly reviewed. Then, main implications of solarising such a technology have been investigated. This section includes the state of art of heat transfer studies in solar rotary kilns and employed simulation methodologies and an overview of the developed prototypes. Among the reviewed solar prototypes, it is presented a novel one which was designed and operated by the authors of the present work. It is also included an experimental assessment that compares a rotary performance with a packed bed configuration, exhibiting how the rotary movement improves the particles heating up and favours their reaction. Finally, some practical conclusions on the design and operation of solar rotary kilns are remarked and an analysis of their main limitations is presented.

2. Rotary kiln technology

Rotary kilns are cylindrical containers that rotate around the longitudinal axis. Generally, they work in a continuous mode. Particles are introduced at one of the ends and are extracted at the other one. Usually there is a gas passing in counter flow. In some other cases, the gas and the solids are in co-current flow. Rotary kilns can have a certain inclination, s, or be horizontally positioned (s = 0). A slight inclination favours the particles axial movement. In the radial directions, particles movement depends mainly on the rotational speed, N, and the fill ratio, $FR\%$, (percentage of reactor volume occupied by the particles). Fig. 1 shows the scheme of a typical industrial rotary kiln. Mellmann (2001) defined three basic forms (slipping, cascading, cataracting) and seven subtypes to classify the transverse motion of solids in rotating cylinders. Previously, Henein et al. (1983) had reported a similar classification and they introduced the bed behaviour diagrams, where different types of bed motion were represented for a certain kind of particles as function of the Froude number, Fr, and $FR\%$. As can be seen in Eq. 1, Fr depends only on the rotational speed and the internal radius of the cylinder, r; g is the gravitational acceleration. When Fr is equal to one, centripetal and gravitational acceleration are equal, and the bed motion corresponding to the centrifugal subtype is achieved. Other bed motions have Fr minor than one.

The type of particles and their characteristics (size, shape, density, angle of repose) also affect the transverse motion inside a rotary cylinder (Boateng and Barr, 1996). Rolling and cascading subtypes in Mellmann classification are the most used behaviours for industrial applications. In the rolling mode, the solid material lines the bottom of the inner wall of the reactor up to a certain height and then, the particles roll down on the upper surface of the bed. Thus, the particles that roll down constitute the active layer, while the particles that rotate as rigid body with the wall of the cylinder constitute the passive layer. The so-called “bed height”, h, (see Fig. 1) remains constant with the rotation and, for a certain speed, the dynamic angle of repose, θ_d, is constant too. From a certain $FR\%$, a core of static particles appears in the central region of the bed, and inside it, mixing is not achieved. Analogously,

when particles with different size or density are introduced inside the reactor, smaller and more dense particles segregate and form a static core (Boateng and Barr, 1996). To solve this problem, some rotary drums present dams, lifters, paddles or fins. Dams increase the level of the solid at the end of the cylinder and, as consequence, particles remain longer inside the reactor, while lifters or fins provoke a sort of particle curtain inside the cylinder that improves particle mixing and heating (Boateng, 2008).

Another fundamental parameter that characterises rotary kilns is the residence time, τ, that indicates the particle permanence inside the reactor. It depends only on geometrical and operation parameters. Its value can vary from few seconds to several hours. Many experimental correlations have been proposed to predict the mean residence time in rotary cylinders. Renaud et al. (2000) proposed a quite complex model to calculate the residence time in industrial rotary dryer. They improved the modified Cholette-Cloutier (1959) model realised by Duchesne et al. (1996). These models discretised the kiln in several units along its longitudinal axis and for each unit, two different zones (an active and a dead one) were taken into account. In the active zone, mass exchanges between a unit and the following one were allowed, while in the dead zone mass exchanges were permitted only with the active zone of the same unit. With this method, differences between simulated residence times and experimental measurements were lower than 5.1%. In the same work, Renaud et al. (2000) compared some of the most used correlations that were based on pilot-scale rotary dryers and they found that most of them underestimated the average residence time.

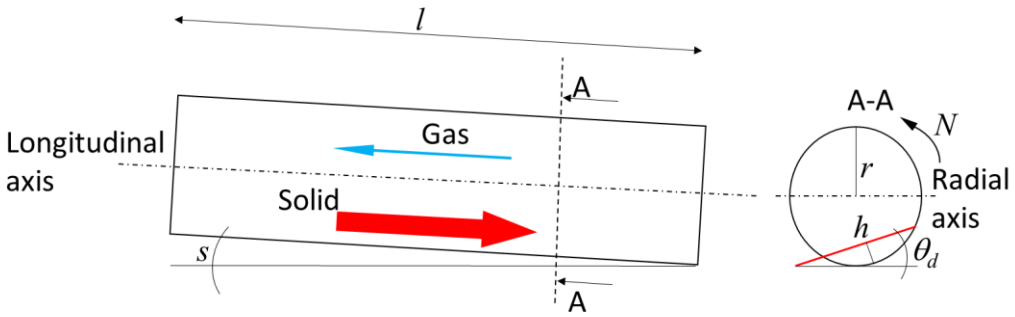

s: slope
l: length of the drum
r: inner radius of the drum
N: rotational speed
h: bed height
θ_d: dynamic angle of repose

Fig. 1. Scheme of an industrial rotary kiln.

$$Fr = \frac{\omega^2 r}{g} = \frac{(2\pi N)^2 r}{3600 g} \qquad (1)$$

$$\tau = \frac{78912\, h^{0.24}}{(tan^{-1}\, s)^{1.02} N^{0.88} (\pi r^2 F)^{0.072}} \qquad (2)$$

In particular, the correlations predicted residence times from 4 to 8 times smaller than measured data in industrial-scale rotary kilns. From that study, the correlation proposed by Sai et al. (1990) resulted one

of the simplest and precise one, achieving a residence period only 1.2 times smaller than real data. Eq. 2 corresponds to Sai's mean residence time correlation, where F is the charge rate per unit of cross sectional area in kg s^{-1} m^{-2}, and N is the rotational speed in rpm.

Operative temperature ranges for rotary kilns can vary from few degrees over ambient temperature to almost 2000 °C (Mastorakos et al., 1999). In order to resist to such high temperatures, internal linings are usually made of refractory bricks or dense castable refractory. Conventionally, the heat to raise the temperature is provided by fossil fuels. The energy required is introduced into the furnace directly by the flame generated in a burner, which heats the solid reactant and the oven walls. In some other cases, the kiln and the burner are separated and the kiln is fed with combustion gases to increase the temperature of reactants. Rotary tube furnaces (indirect fired kilns) can operate at temperature higher than 2400 °C (Boateng, 2008). These furnaces usually consist in graphite tubes where the reactants flow inside the tube, while the heating gas is external to the tube. Commercially, some vendors declare to produce rotary tube furnaces that can work with temperatures up to 3000 °C (Harper-International, 2016). Thus, the heat transfer in rotary reactors has complex mechanisms and it depends on the kiln configuration. In the most of the kilns it is produced by a combination of radiation, convection and conduction between the gas, the particles and the wall of the kilns. Furthermore, because of the kiln rotation, heat transfer is complicated by particle mixing inside the solid bed.

Several models have been proposed to predict the thermal behaviours of rotary kilns (Boateng and Barr, 1996; Brimacombe and Watkinson, 1978; Dhanjal et al., 2004; Gorog et al., 1983; Iguaz et al., 2003; Mastorakos et al., 1999; Palmer and Howes, 1998; Watkinson and Brimacombe, 1978; Yang and Farouk, 1997; Yang et al., 1999; Zhang et al., 2008). For instance, Brimacombe and Watkinson (Brimacombe and Watkinson, 1978; Watkinson and Brimacombe, 1978) employed a pilot scale rotary kiln (5.5 m length and 0.406 m inner diameter, $i.d.$,) filled with inert sand to do a comprehensive analysis of thermal transfers. Fifty-two thermocouples were inserted inside the kiln to monitor the temperature of the gas, the solid and the walls along the kiln axis. A comparison between thermal model and experimental results was conducted for different operating conditions. In their experiments, they reached a maximum temperature of almost 800 °C for the gas, solid and walls. Because the measured particle and kiln wall temperatures were very similar, radiative and conductive heat transfer between solids and walls were neglected in the model. They concluded that the heat transfer to the bed is a two-stage process: first, heat is transferred from the gas to the particles on the bed surface and then mixed inside the bed due to particle movement. Furthermore, the most significant effect of rotary kiln heat transfer is the convection from the hot gas to the solid, which controls almost 70% of the energy transferred to the particles. Radiation from the gas to the particles represents less than 30% of the heat absorbed by the solid. Moreover, the heat flux from the gas to the solid bed is ten times greater than the heat flux to the kiln walls. They also remarked the importance of working in rolling mode to improve the heat transfer between the gas and the solid bed.

Boateng and Barr (1996) developed a quasi-three-dimensional, 3D, model for inert particles, which was obtained by the combination of a two-dimensional, 2D, thermal model for a transverse section of a

rotary kiln and a mono-dimensional, 1D, axial model. Firstly, the mono-dimensional model was validated with experimental temperature measurements along the axis of a pilot rotary kiln with the same size of the one reported by Brimacombe and Watkinson (1978). Then, the results were used as boundary condition for the 2D model. In this way, the authors generated temperatures profiles for different ranges of rotational speed (0-2 rpm), particle size (0.297–3.36 mm), gas velocity (1.41-2.53 kg/s), freeboard gas temperature (600-1200 °C) and fill ratio (12% and 27%). As main conclusions, the authors found that isothermal profiles were achieved in the transversal sections when spherical particles with the same size were introduced in the reactor and the rotational speed was sufficient to generate rolling mode conditions with the lowest $FR\%$. Otherwise, when segregated bed arose, temperature gradients of over 200 °C could be achieved in the transversal section.

Palmer and Howes (1998) presented a heat transfer model for the drying of an alumina de-watered slurry in a rotary kiln 132 m long and 4.2 m $i.d.$ The model incorporated a combustion profile to simulate the non-instantaneous combustion process. The drying of the feed proceeded from the surface to the interior of the bed and temperature profile of solids changed along the axis of the kiln. The maximum gas temperature considered in the model was 1500 °C. Authors concluded not all the thermal energy went into the latent heat of vaporisation needed for the drying process, but a certain amount of the heat increased the temperature of the feed solids. Moreover, convection was the main heat transfer mechanism for the drying of the alumina.

Mastorakos et al. (1999) analysed a coal-fired rotary cement kiln (4.1 m $i.d.$ and more than 80 m in length) and realised a CFD predictions of its thermal behaviour. To study the radiative heat transfer, they used a particular module based on Monte Carlo method that was integrated with a three-dimensional flow module. In their work, they considered a maximum temperature of almost 2000 °C inside the kiln and in contrast to other authors, they found that the contribution of convection to the overall heat transfer from the flame to the solid bed was almost negligible. This is probably due to the higher temperature range considered for the kiln. However, the authors suggested the discrepancy of their results with Carvalho et al. (1995) was due to the value of the gas parameters used for the calculation of the convective heat transfer. In particular, Mastorakos et al. used local values for the gas temperature and velocity, while Carvalho et al. employed average values over the cross section.

Dhanjal et al. (2004) proposed a two dimensional mathematical model for the heat transfer in the transverse plane that was based on experimental results of a pilot-scale batch kiln. The cylinder had an internal diameter of 0.4 m, a length of 0.6 m and the rolling mode was maintained by keeping its speed to 1, 2 and 3 rpm according to the trial. The experiments consisted in heat up inert sand from ambient temperature to almost 775 °C. Four thermocouples measured the temperature inside the sand bed at different depths. To simulate the conductivity in the active layer, a mixing conductivity was calculated by fitting real temperature with simulated ones. On one hand, results showed that mixing conductivity was 5 times higher than the bulk thermal conductivity of the material. On the other hand, a temperature

gradient was noted along the bed height, in contrast with the objective to obtain particles with a homogenous temperature.

Yang and Farouk (1997) studied the heat transfer in a rotary kiln filled with granular solid particles. Following the methodology proposed by Boateng and Barr (1996), they developed a quasi-3D model. The heat flux on the bed surface was determined in the 1D model and it was employed as boundary condition for the cross-sectional model. The model was validated with experimental data obtained by Tscheng and Watkinson (1979) in a pilot rotary calciner (2.5 m in length and 0.19 m $i.d.$) which worked at low temperatures (less than 200 °C). Among the results, the authors highlighted that the particle temperature in the cross sections was not uniform and the convective heat transfer was the primary mode for bed heating.

As can be inferred so far, well-mixed beds can be achieved in rotary kilns, but not for all working conditions. In order to achieve uniform particle temperatures, the rotary kiln has to work in rolling mode. Furthermore, to avoid segregation, particles should have the same size and shape; segregation can be minimised with low $FR\%$. Introduction of internal elements such as paddles, fins or lifters can improve particle mixing.

For the calculation of the residence time of particles inside a rotary kiln, several models have been proposed. However, as general conclusion, it is not possible to apply the correlations obtained in small kiln prototypes to the industrial ones. In particular, the geometrical relation between particles and kiln walls is not respected when the kiln is scaled-up and, according to Renaud, correlations deduced with small kilns are not valid. Thus, specific models have to be developed for each case if it is needed a good prediction of the residence time.

Related to the thermal behaviour inside classical rotary kilns, there is no concurrence among the reported conclusions. Some authors (Palmer and Howes, 1998; Watkinson and Brimacombe, 1978; Yang and Farouk, 1997) declared that convection from the solid to the gas is the main form to heat up the solid, while radiative heat transfer from the flame to the particles represents only a partial contribution to the overall heat flow absorbed by the solid bed. Instead other authors (Mastorakos et al., 1999; Shahin et al., 2016) declared that convective heat transfer is negligible and the overall heat transfer is almost totally due to radiation. These discrepancies in the results could be due to some factors. The kiln working temperature can be very different from case to case and at higher temperatures, radiative heat transfer is dominant. Moreover, the geometry and the heating mode of the kiln can influence the overall heat transfer. In a long kiln, radiative heat transfer will be more preponderant in the region close to the flame and it will decrease along the kiln. Close to the gas outlet, convective heat transfer will be higher. In indirect fired kilns, the process of burning occurs outside the kiln and because of the very low value of emissivity of the combustion gases (Ludwig et al., 1973), convection will be the main contribution to the overall heat transfer.

3. Industrial applications

Since the end of 19th century, rotary kilns have been employed for the production of cement. Usually, they have been utilised to conduct calcinations of a variety of products as sands, limestones, aggregates and gypsum. Nowadays, the use of rotary kilns is widely extended in many industries, including food, pharmaceutical industry, mineral processing, metallurgical foundries, treatment of wastes, etc.

In the field of cement industry, Boateng (2008) classifies rotary kilns in wet and dry, short and long, cooler and dryers, and direct and indirect fired kilns. Wet kilns are usually fed with slurry materials and are the longest ones. They can reach lengths of more than 150 m. Because of their low efficiency, they are not frequent and they are more used in food and paper industry. Otherwise, long dry kilns, which have higher efficiencies, are typically used for the treatment of lime and lightweight aggregates. Their mean length is about 100 m. In cement plants, short dry kilns have a length in a range of 15-75 m, while indirect fired kilns are the smallest ones employed in this sector with diameters up to 1.3 m. They are used when the contact between gas and solid is not desired and they are useful for several applications as reduction, calcination, oxidation, and carburisation in a controlled atmosphere.

Apart from the use of rotary kilns in cement plant, other applications have to be mentioned. For instance, these devices are employed for the treatment of wastes. Wey et al. (2006) investigated the continuous sintering of fly ash from the urban solid waste and the reduction of the concentration of heavy metals in it (mainly Pb, Cu, Cd and Cr). Working with a pilot-scale kiln (2.10 m long x 0.09 m $i.d.$) in a temperature range of 700-900 °C, they could reduce the concentration of heavy metals in the fly ash. In the same field, Descoins et al. (2005) studied the flow of granular solids in a pyrolysis pilot-scale rotary kiln. The reactor was externally heated, could reach a maximum temperature of 1000 °C and had a 0.21 m $i.d.$ and 4 m in length. Experimental studies on urban waste pyrolysis were also conducted by Li et al. (1999). The kiln, which was heated by an external electric furnace of 12 kW, had an $i.d.$ of 0.205 m and it was 0.450 m long. Through the pyrolysis, gas and coke can be produced with low emissions of dioxin and furan from a wide range of waste materials. Li et al. tested several types of urban wastes (plastic, rubber, wood, cotton cloth, vegetal, etc.) and worked at different temperatures (up to 900°C). Regulating the kiln freeboard temperature, they obtained different compositions and heating values of the produced gases, (mainly CO, CH_4, H_2, CO_2 C_2H_4 and C_2H_6).

Generally, rotary kilns with smaller l/d are employed for pyrometallurgical processes. These kilns can be operated in batch or continuous mode for the extraction and/or melting of different metals as iron, copper, aluminium or lead. For instance, aluminium scrap melting is conducted in rotary furnaces at temperature of about 800 °C. For this purpose, Zhou et al. (2006) reported an industrial scale rotary kiln of 3.0 m $i.d.$ and 6.9 m in length, that rotated at 1.33 rpm with melting time up to 6.25 h. To study metal melting, Zhang et al. (2008) constructed a bench scale rotary furnace that worked in continuous mode with a shell diameter of 0.51 m and a length of 0.72 m.

Other rotary kilns can be found for low temperature applications. For instance, in the agro-food industry, rotary kilns are often small and are used to dry the products. In this field, Iguaz et al. (2003) simulated the dehydration process of wastes of vegetable with air at approximately 200 °C. For a similar application, Kaleemullah and Kailappan (2005), investigated the drying process of red chillies in a rotary dryer (0.3 m long x 0.4 m $i.d.$) in a range of 50-65 °C.

Vijayan and Sendhilkumar (2014) reported a review of the main industrial operations, which generally are conducted in rotary kilns. They defined five types of applications: calcination, manufacturing, incinerator, thermal processes and pyrolysis, and for each one they reported some examples together with their principal characteristics (length, inner diameter, slope, and temperature range). Manufacturing includes cement industry and metallurgy industry. This sector covers approximately 40% of rotary kiln allocation of application level; thermal processing represents the 30% of allocation level, and pyrolysis, calcination and incineration the 15, 10 and 5%, respectively. Vijayan and Sendhilkumar concluded that most of the rotary kilns generally have a slope of less than 5°, the ratio l/d can change from 1 to 30, and the temperature range can vary from ambient temperature to 1500 °C depending on the required process.

4. Solarisation of rotary kilns

Since rotary kilns have been widely employed in industry with success, they have been also considered in solar R&D from decades. Several simulation models have been found in literature devoted to understand the heat transfer mechanisms and the general behaviour of solar rotary kilns. Some prototypes have been designed and constructed with different scales and have been coupled with solar furnaces and solar simulators for experimental demonstration. They have been provided with elements that facilitate the parameters measurement and process tracking. Recently, other studies consider a further feasible implementation of the rotary kiln in a real solar tower plant (Alexopoulos et al., 2015; Gallo et al., 2016). In the following sections, details are given about the cases reported in literature. An analysis of the main limitations of the technology is also presented.

4.1 Developed studies on heat transfer and simulation methodologies applied to solar rotary kilns

The thermal analysis of solar rotary kilns applied to high temperature processes (thermal or thermochemical) requires the study of the fluid flow, the heat and mass transfer, and the chemical reaction. Hence, the computational model developed for that purpose couples these phenomena. Furthermore, in solar rotary kilns, particular attention should be given to radiation heat transfer because it has a significant influence on the thermal process. Thus, different strategies to model the solar radiation on cavity type reactors are found in literature and they can also be implemented in rotary kiln models considered for industrial applications.

The thermal behaviour of solar rotary kilns used in thermochemical applications has been analysed by simulation. One of these applications is the thermal reduction of metal oxides involved in water-splitting thermochemical cycles for hydrogen production. Abanades et al. (2007) designed and simulated a lab-scale solar reactor for the mentioned process with a cavity directly heated by concentrated solar energy

that received continuously injected solid particles. A multiphase model (solid-gas flow) was considered to simulate the reactive particle-laden flow and a discrete phase model was performed by a Lagrangian approach. This model was able to predict temperature and gas velocity distributions, species concentration profiles, particle trajectories and conversion rate from the reaction degree of completion. In addition, the influence of the incoming solar radiation was implemented by a flux density profile to define the heat absorbed by the inner cavity wall because it was neglected on the remaining solid parts. In this case, the walls were assumed opaque in the radiative transfer equation, while the inert gas was transparent to the radiation. Furthermore, the effect of the discrete solid particles was included in the radiation model. The radiative transfer equation was solved in the discrete ordinates grey-radiation model, considering absorption, emission and scattering of the particulate phase (Abanades et al., 2007).

In previous studies, simulation models focused on a most accurate representation of the radiative exchange. Sammouda et al. (1999) analysed theoretically and experimentally the different phenomena of mass and heat transfer interchange amongst the sand particles heated at temperatures higher than 1000 °C by concentrated solar radiation. Fig. 2 shows the heat flow paths in a solar rotary kiln full of granular solids, including the influence of the heat transfer mechanism on the solid. As described in this figure, the solid material can be heated by the incident solar radiation and by the heat transferred from the kiln walls that come into direct contact with the granular solid. However, the heat flux received is also transferred to the gas present in the cavity. Hence, this kiln has been conceived for inert reactions of system composed for gas (air) and particle solids, where the gas is considered transparent for solar rays. The heat flux captured depends on the movement of particles in the cavity according to dynamical parameters that characterise the operating mode of the rotary kiln. Solid mixing-processes have substantial effects on overall heat-transfer rates and the control volume of the solid load (so-called burden solid in Fig. 2) is defined by the kiln inclination angle, v, the mass-flow rate of granular solids, $\dot{m}_s$ and the kiln rotational velocity, ω. For the condition of well-mixed solids, it was assumed that the solid outer layer and the inner part of the solid load have a similar temperature. Thus, the solid was considered as a porous medium where the heat transfer coefficient between granular solids and the air is infinite, and particles of the same cross-section have the same temperature (Sammouda et al., 1999). Besides, the kiln walls collect the concentrated radiation and transfer the heat to the granular solids. Therefore, their thermal behaviour should be analysed by coupling radiative, convective, and conductive phenomena in the rotating-kiln area located at the concentrator focal point (see Fig. 2). The absorption and emission of solar radiation at the receiver surface are defined by complex functions for wave length and direction. However, Sammouda et al. simplified the study of these processes by considering grey, diffuse and opaque kiln walls with radiative properties independent of the temperature.
Thus, according to Fig. 2, the temperature of the lateral wall only depends on the longitudinal axis and the one of the bottom wall is dependent on the radius. In fact, the kiln rotation homogenises the radiance and allows the achievement of uniform temperature in each ring-shaped segment of lateral and bottom walls (Sammouda et al., 1999).

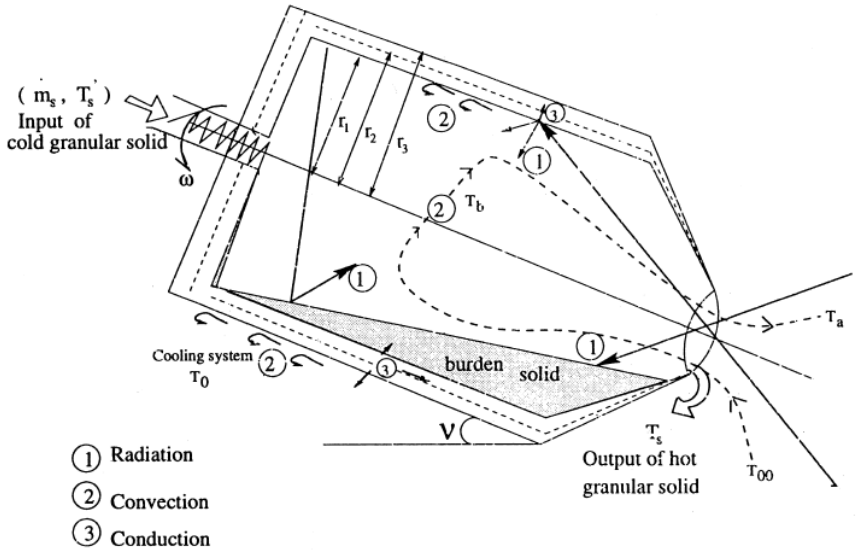

Fig. 2. Heat transfer of a solar rotary kiln with solid particles (Sammouda et al., 1999).

The solar-driven dissociation of ZnO particles at 1600-2136 K range was simulated by Schunk et al. (2009) with a transient heat transfer model that included Monte Carlo ray tracing method (MC) to study the radiative transfer in a horizontal rotary reactor. This study was developed to analyse the thermal performance of the thermochemical reactor with semi-batch feed cycles of ZnO particles. In this model, the effective thermal conductivity is regarded as the sum of the radiative and conductive contributions which were obtained by the Rosseland diffusion approximation and by the results from a previous research, respectively, considering a porosity of zero for the porous packed-bed. The convective heat transfer coefficients at the inner surfaces of the cavity, external walls and quartz window were obtained by Computational Fluid Dynamics (CFD) simulations and correlations found in literature, defining the angular velocity and characteristic lengths. Furthermore, the radiative exchange in the cavity is modelled by assuming directional incident solar radiation and diffuse emission by the cavity walls. In this case, the net heat source coming from the solar radiation was modelled by MC to obtain the net radiative flux arising from radiation emitted by the cavity walls. Thus, this model offers a more detailed description of the radiative exchange in the solar reactor.

Tescari et al. (2013) proposed a later thermal model for rotary kiln reactors, considering the reactor aperture as a fictive surface at an imposed equivalent temperature in order to decrease the computational cost whilst maintaining the accuracy of the solution. The feed gas was regarded transparent to radiation and it was taken into account the radiative transfer between inner walls of the reactor and to the aperture, the convective transfer to the gas passing through the cavity of the reactor, and conduction through the insulation towards the external wall. At the outer walls, the heat flux comes from radiative and convective transfer. Hence, the convection coefficient was calculated by empirical formulae for horizontal rotating surface. Two radiation models were considered in the CFD simulations performed. The discrete ordinates method (DO) was used to evaluate the importance of the quartz-window effect, and the surface-to-surface model (S2S) was selected for the optimisation of the

calculation time when the effect of semi-transparent absorbing media is neglected. Thus, the reactor aperture was modelled as a volume of quartz surrounded by transparent surfaces defining its optical properties for the DO model or as an opaque fictive surface at a fixed temperature equivalent to the incident heat flux for the S2S model. The results obtained with both models showed the same tendency, and thereby the S2S model was used to optimise the reactor design (Tescari et al., 2013).

In the most recent study, a special programming language was chosen for the simulation of solar aluminium recycling in a rotary kiln (Alexopoulos et al., 2015). The model consists of unsteady state one-dimensional heat transfer equations for the wall elements, dynamical energy balances for the components located at the reactor cavity (aluminium, salt and air), and additional equations for material properties and heat transfer. It was assumed that the gas does not absorb any solar radiation and transports heat only by convection. The front and back surfaces and the uncovered cylindrical inner wall were directly irradiated by the concentrated sunlight. The aluminium was covered by the salt (mixture of NaCl, KCl and CaF_2) and convective transfer was considered between both materials, to the ambient air, and to the front and back cover; the required heat transfer coefficients were obtained from literature. Radiative heat transfer inside the rotary kiln was calculated according to the latter method, which considers laws of Lambert and Kirchhoff, front and back openings as black bodies, the gas as transparent medium to radiation (low concentration of H_2O and CO_2), the inner wall and salt flux as diffuse-grey surfaces, and negligible scattering. This method divides the enclosed volume of the kiln into a number of zones with uniform thermal distribution and radiative properties (Alexopoulos et al., 2015).

The above mentioned information about the different simulation methodologies developed for solar rotary kilns shows that the assumptions considered for radiative transfer mainly depend on the thermochemical process accomplished, the computational cost and the desired accuracy.

4.2 Review of developed prototypes of solar rotary kilns

The earliest studies on solar rotary kilns date from 1950's and 1960's and they were developed by Trombe and Foex at the CNRS 1 MW solar furnace in Odeillo (Trombe and Foex, 1954; Trombe, 1963, 1973) for the thermal treatment of different substances. They employed a water cooled rotary kiln with 500 litres of capacity to melt refractory oxides and produce bulk materials. The rotary reactor was also employed to purify alumina and quartz. It was able to operate both in batch and continuous mode and it rotated at sufficient speed so that the material to be treated could be maintained against the wall by centrifugal force. A United States Patent was granted in 1957 to Felix Trombe for the design of the solar rotary kiln.

Another of the first solar rotary kilns reported in literature was designed also in Odeillo, at Laboratoire d'énergétique solaire of CNRS (today it is called CNRS-PROMES), in 1979 (Flamant, 1980; Flamant et al., 1980). The device was tested for two processes. The first one was a thermal process consisting in the heating of refractory materials at 600-1300 °C. The second process involves a thermochemical transformation, particularly the decarbonation of calcite at 850 °C. The reactor consisted of a cylindrical

drum with slope of 5°. The inner wall was a tube made of refractory material. The kiln included an insulation layer, a water cooling jacket and an external housing. Its scheme is shown in Fig. 3. The refractory tube was 0.09 m in length and 0.02 m inner diameter. The residence time of the particles in the reactor could vary between 20 s (25 rpm) and 120 s (4 rpm) depending on the rotation speed. The reactor was conceived to operate in continuous mode. Reactants were feed through the rear and removed through the front. The solar radiation impinged in the front side, where an aperture was placed, and entered in the kiln. Since the reactor length was more than four times its diameter, a high radiation angle of incidence contributed to the appearance of high thermal gradients. Authors searched for the cavity effect within the reactor design, because they expected a total absorbance of the system close to one. However, there is not an aperture of lower diameter that could help to avoid radiation losses and a heterogeneous distribution of the radiation profile probably takes places along the tube. The cavity effect was not present inside the reactor chamber and the temperature was not uniform. Flamant et al. (1980) reported an axial thermal gradient along the reactor walls of 10^4 °C/m. Additionally, they informed maximum and minimum temperatures of the treated material of 1500 °C and 300 °C respectively. For the thermal process, Flamant (1980) reported a maximum efficiency of 30% which was calculated as the rate of the sensible heat that gained by the refractory material to the power intercepted by the reactor aperture. For the thermochemical process, the efficiency was 7%. In this case, the energy gained by the material was the sum of the sensible heat and the reaction enthalpy. Both processes were also performed using a batch fluidised bed reactor and higher efficiencies, both thermal and thermochemical, were obtained (40% and 20% respectively). However, lower temperatures were achieved with the fluidised bed. It seems that the high thermal gradients in the rotary kiln penalised the material energy absorption while the mixing conditions found in the fluidised bed improved it.

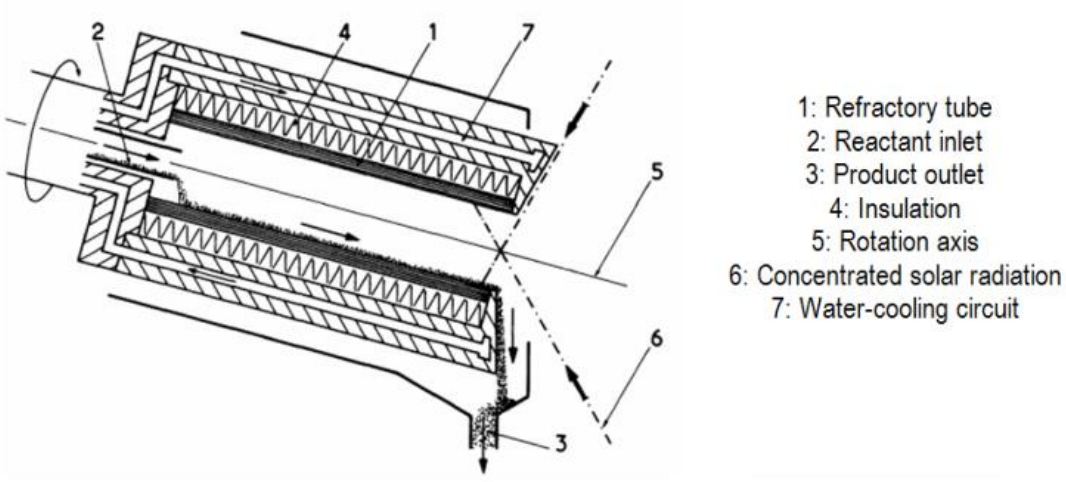

Fig. 3. Scheme of the Flamant's rotary kiln. It consists in a sloped refractory drum, and insulation layer and a water cooled housing. Radiation was concentrated at the front side of the kiln (Flamant et al., 1980).

Meier et al. (2004) performed an extensive work on the $CaCO_3$ calcination to produce CaO and CO_2, which was supported by the company Qualical belonging to the lime sector. To that end, they designed and constructed a rotary kiln for 10 kW solar power input and it was tested in the PSI solar furnace. The reactor housing was a cylinder of 0.6 m length and 0.35 m in diameter. Although the kiln was placed in horizontal position, the reaction chamber was an insulated refractory cone with an angle of 5°. The reactor was tested in PSI's solar furnace. It worked in continuous mode by feeding particles through the top of the rear part and discharging the solid products through the front part. By means of the feeding rate and rotation speed, one was able to control the residence time. Authors searched for conditions that allowed a rolling motion of the particles. They performed tests with rotational speed of 2-7 rpm and they concluded that the highest values gave rise to preferred behaviours. Experiments were carried out under steady-state conditions. The rotary kiln was first preheated about 1.5-2 h. Then, authors performed typical experiments of 30 min with a constant reactant particle flow rate. From a mass balance, it was found that some of the fed mass was missed. Part of it remained in the reactor and another part left it through the aperture. The reactor suffered some thermal shock which authors described as no severe and experimental campaigns were not affected. The obtained calcination degrees exceeded 98% and the reported temperatures in the kiln were up to 1400 K (Meier et al., 2004). Authors employed the rate of reaction enthalpy of CaO at 298 K to the solar power reaching the reactor to calculate the solar to chemical efficiency. Typical values were 13% with a maximum of 20%. To increase the efficiency, authors proposed to partially recover the sensible heat of products and to improve the insulation. However, they found that around 50% of the solar power input was unaccounted. Likely sources of such unknown heat losses could be free convection and hot calcined powder leaving the reactor through the aperture. The calcined power had white colour and formed a cloud around the reactor aperture that reflected and absorbed a significant part of the solar power. To avoid this, authors proposed an indirectly heated multi-tube rotary kiln in a further work (Meier et al., 2005a, 2006). It consisted in several tubes inside which the reactant was fed. These tubes were distributed around the wall of a cylindrical cavity. The 10-kW reactor worked in the same range of temperature than the other one and could treat 4 kg/h of limestone particles. The reactor reached an efficiency of 30-35%. The authors proposed the scale-up at 0.5, 3 and 20 MW (Meier et al., 2006) and they estimated the cost of solar lime production about 2-3 times the price of conventional lime.

After several studies on thermochemical storage based on cobalt redox pairs, DLR adapted a rotary kiln to perform the process under concentrating solar energy (Neises et al., 2012). They highlighted that, in this way, the storage material was directly heated by solar radiation and a good mixing of the particles would guaranty a homogenous temperature distribution during the endothermal step. The concept proposed by Neises et al. (2012) should be accompanied by other plant components to carry out the recovering of heat off sun. The original rotary kiln was designed more than one decade before and was tested for detoxification of hazardous materials and aluminium recycling (Funken et al., 1999; Glasmacher-Remberg et al., 2001). Fig. 4 shows a scheme of the device when it was employed to recycle aluminium. The figure was taken from Alexopoulos et al. (2015). It consisted of an insulated crucible furnace made of silicon carbide (0.4 m length and 0.2 m diameter), which was placed inside an insulated

metallic housing rotated by an engine. The solar radiation entered into the crucible furnace through the aperture, which had a diameter of 0.08 m. In an experimental campaign in DLR solar furnace, authors estimated that 70% of the concentrating radiation entered into the kiln. They suggested employing a secondary concentrator to improve the rate of useful radiation. It was separated from the reactor aperture by a narrow duct which probably helped to maintain it free of particles deposition. The reactor could also incorporate a quartz window in the entrance plane of the secondary concentrator in order to work with adjustable compositions of gas phase inside the chamber. In this case, carrier gas was introduced behind the window, helping to keep it clean of depositions as well as the secondary concentrator. Differently to the previously reviewed prototypes, this rotary kiln operates in batch mode. While the reactor rotated at 20 rpm for treating hazardous materials, rotational speed selected in thermochemical storage application was 6 rpm. Since the adequate rotational speed depends on the amount and type of charge, versatile prototypes should be provided with rpm controller. The reactor was turned out of the horizontal plane by 13°. With this arrange, no significant detriment would be expected in the radiation acceptation while it is possible to increase the amount of reactant in the charge. Some thermocouples were in contact to the wall while others were immersed in the particles bed. In this way, temperatures at different points of the reaction chamber were measured. Authors highlighted the need of a good mixing of the particles to improve the homogeneity of the bed and the process performance. They proposed to operate with high rotational speeds and include stirring elements in the kiln.

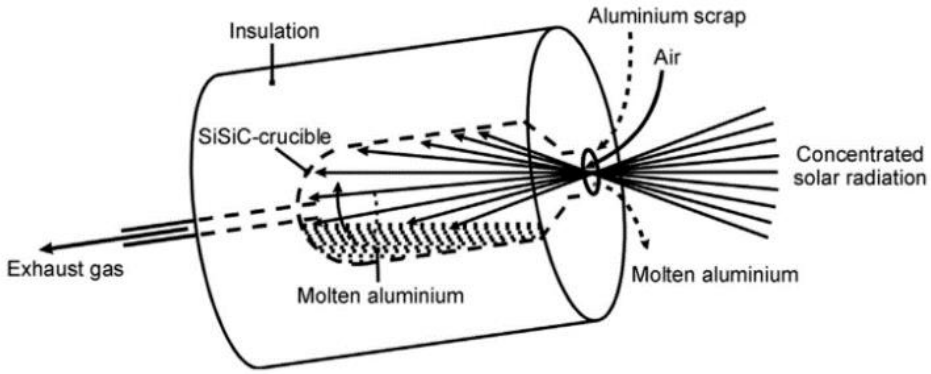

Fig. 4. Scheme of the DLR rotary kiln published by Alexopoulos et al. (2015). It was composed of an insulated crucible, a frontal duct and a housing.

The authors of the present work developed a rotary kiln to study the thermochemical storage of solar energy based in copper oxides (CuO/Cu_2O thermochemical pair) (Alonso et al., 2015). It consisted of an insulated ceramic cavity of 0.058 m inner diameter, 0.067 m outer diameter and 0.074 m in length, closed by a stainless steel skeleton. The reactor was provided with a water-cooled quartz window of 0.210 m diameter and 0.008 m thick. No slope was given to the reactor drum. Carrier gas was injected into the reactor by four radial perforations equally spaced across a frontal cone that separated the window and the cavity. After passing the reaction chamber, carrier gas left the cavity through a duct placed at the reactor back. The ceramic cavity was connected to an axis and a gear assembly so that it

was able to rotate. Temperatures at various locations of the reactor body were measured with thermocouples. In order to measure and record temperatures at rotary parts, it was employed a wireless acquisition device that rotated together with the reactor. An experimental work of CuO/Cu_2O redox cycles were carried out with a gas flow rate of 10 Nl/min and rotation speed of 4 rpm. The HoSIER solar furnace facility of IER-UNAM was employed. CuO was first reduced in argon and conversions around 80% were achieved. Then, reduction-oxidation cycles were performed in presence of air, which disfavoured the conversion rate. Results indicated that CuO/Cu_2O cyclability was feasible but an optimisation of the rotary reactor operation parameters was required. Parallel to the studies on thermochemical storage, the authors devoted to analysing the solar reactor concept and operation mode. A preliminary investigation stage aimed to compare the rotary device with a static one was carried out. For such a comparison work, the described solar reactor was employed. If the drive gear was disabled the reaction chamber remained static. Fig. 5 shows a photograph of the solar reactor and a sketch where rotary parts are highlighted in red. Note that these parts do not rotate when working under stationary mode.

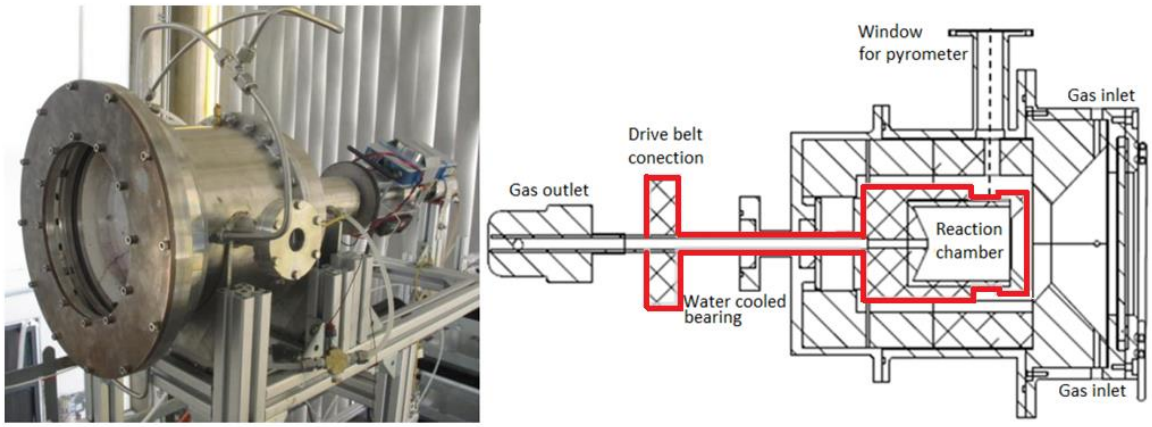

Fig. 5. a) Photograph of the rotary solar reactor installed in the focal zone of the solar furnace (window cooling circuit removed). b) Sketch of the solar reactor with rotary parts marked in red.

In case of stationary experiments, sample was arranged in a packed bed by using a rod made of synthetic alumina (0.014 m inner diameter, 0.025 m in length) as sample holder. Such an arrangement was selected for this comparative purpose because it has been employed in several previous works. It eases the measurement of reaction parameters, such as reaction temperature, or evaluating the interaction between reactants and radiation (Alonso and Romero, 2015b) . With this arrangement, it is also possible to develop parametric analysis and kinetic studies (Alonso et al., 2013; Moller and Palumbo, 2001; Schunk and Steinfeld, 2009). To compare rotary and static behaviours, the solar reactor was operated with and without connecting the gear, under the same working conditions (10 g of reactant, 10 Nl/min of argon as carrier gas), in the IER-UNAM solar furnace. The rotational speed set for rotary mode was 4 rpm. Reductions of two different oxides, Mn_2O_3 (powder, 99.9% -325 mesh from Sigma Aldrich) into Mn_3O_4 and CuO (98% powder, <10 µm, from Sigma Aldrich) into Cu_2O were performed. Fig. 6 shows both types of samples (the material in the picture is CuO) prepared to be

introduced in the reactor. In order to follow the progress of the reductions, the oxygen concentration was measured at the reactor outlet.

Fig. 6. Samples of CuO prepared to be introduced into the solar reactor: packed sample to be used under static working mode and powder sample to be used directly under rotary working mode.

Qualitative observations based on the physical change of the samples showed that the rotary mode lead to better results in terms of reactant conversion. Fig. 7 compares the aspect of the samples considered in Fig. 6 after being treated. In stationary mode, a colour change was only observed in the front layer of the sample (oriented towards the radiation). In that region, a partial reduction took place and material had also slightly melted. A small amount of metallic copper was also found at the front, indicating a second reduction from Cu_2O to Cu. However, the middle and the rear of the sample had not been converted because the temperature in those regions did not reach the reaction temperature. The boundary that separates the reduced part from the inactive region is clearly observed in the right picture of Fig. 7a. All these findings were corroborated by XRD analysis. The measurement of delivered oxygen indicated that the fraction of converted CuO was only 16%. However, under rotary mode, the heat transfer between the gas and solid phases was improved and the particle temperature was homogeneous. Moreover, the particle motion helped to decrease their sintering and melting (Neises et al., 2012). Thus, 80% of conversion was achieved, as indicated before, for CuO reduction. In Fig. 7b, it is observed how the material has adopted a colour close to the red of Cu_2O. Although some particles were lightly adhered to the reactor wall, neither fusion nor sintering was detected. Then, the solid product could be completely recovered from the reaction chamber. The particles had formed small spheres or balls with a range of diameter about 0.5-3 mm. Most of them presented a weak compaction, so that the original consistence of the particles could be restored with a small compression.

Studies on manganese oxides also determined a better performance of the rotary kiln mode. Due to the lower transition temperature of this case (theoretical transition temperature is 900 °C as compared with 1120 °C for CuO), Mn_2O_3 samples were almost totally converted in both operation modes. However, the treatment time required for stationary experiments was four times higher than the one for rotary mode.

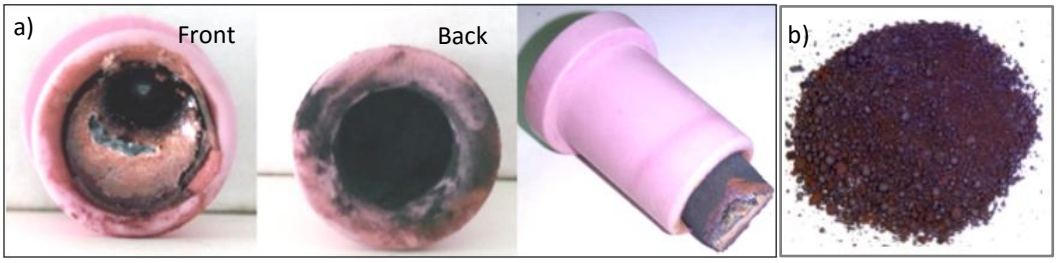

Fig. 7. a) Different views of the packed sample corresponding to Fig. 6 after the thermal treatment. b) Powder sample of Fig. 6 after the thermal treatment. Note that black is the typical colour of CuO and red-brown of Cu_2O.

Sammouda et al. (1999) presented a very complete study on a solar rotary kiln employed as a sand boiler. Their main effort was put in developing an accurate heat transfer model to understand the specific phenomena that take place inside the kiln. The model was validated by experimental demonstration that was carried out in the 1 MW solar furnace of Odeillo (France). The rotary kiln was conceived to heat sand that was further employed to heat air by using a heat exchanger. The sand type was dark quartz in order to favour the absorption of solar radiation. The kiln was a closed cavity with an aperture that served as entry for solar radiation and as exit for hot sand. The cavity was constituted with refractory fibres. The reactor was 1.20 m in length and 0.64 m in diameter (see Fig. 2). It rotated around the longitudinal axis and it can be inclined relatively to the horizontal. A water circuit cooled the external face of the kiln. In the experimental campaign which authors carried out to validate their numerical model, they analysed the influence of the operating parameters on the axial temperature profiles of solid: rotation speed, sand mass flow rate (410, 550, 600 kg/h), inclination angle (5-8°) and solar radiation (141, 160 kW). For temperature measurement, an optic pyrometer was used. Authors notified the impossibility of measuring walls temperature due to the geometric form of the kiln and because the presence of concentrated radiation does not permit to place instruments inside the kiln. The employment of thermocouples was not reported.

A different type of solar rotary reactor has been considered in PSI and two different prototypes have been constructed on the basis of the same concept. They were developed for the solar thermal dissociation of ZnO (solid) into Zn (gas) and O_2 (gas). In a previous review work it can be found a complete summary of the ROCA (Haueter et al., 1999; Palumbo et al., 2004) and ZIRRUS (Müller et al., 2006, 2008; Schunk et al., 2008, 2009) reactors conception, design, testing and improvement (Alonso and Romero, 2015a). Here, the objective is to compare the concept thought up by PSI researchers with other rotary kilns found in literature. In fact, PSI concept has common elements with other reviewed solar rotary kiln: a rotary drum which can be considered as a cavity where the radiation enters and heats the reactants. However, attention must be brought to important differences:

- The PSI solar reactors include a water cooled quartz window that allows operating under controlled atmospheres. In this way, processes that need particular atmospheres can be studied, extending the field of application of these reactors. The window is kept cool and clear of particles because the gas

stream enters in the cavity tangentially to the window. Moreover, by controlling the reactor atmosphere, the gas composition can be analysed at the outlet. Such a parameter can be very useful for different studies, for instance, reaction kinetics evolution or chemical conversion. This characteristic has been found in other but not in all the solar rotary kilns.

- The particles bed motion, due to very high rotation speed (Müller et al. (2008) considered an angular velocity of 120 rpm while Schunk et al. (2009) indicate a range of 30-120 rpm), is centrifuging, what means Fr equal or higher than 1. The bed material rotates with the drum wall. The same idea was found many years ago with the solar rotary cavity developed by Trombe (1973). Note that industrial rotary kilns usually work with Fr well below the centrifuging mode and probably the cascading mode as well.
- In the case of PSI solar rotary reactors, the ZnO decomposition process give rise only to gaseous products. That means that the solid layer of reactants, which is fixed on the reactor wall, is converted in gaseous products while the reactor is irradiated. Such a characteristic seems to fit well with a centrifuging bed motion.
- Due to the particularity of the bed motion, porosity and extinction coefficient of the particles bed play an important role in the reactor performance.
- The reactants form a layer inside the reaction chamber that protects the cavity walls from thermal shocks. With this arrangement temperatures close to 2000 K can be achieved without damaging the cavity.
- It was noticed the need of avoid the diffusion of atmospheric air into the reaction chamber. With the improvement of PSI prototypes, researches pay attention to the use of hermetic seals. Moreover, they apply a small overpressure inside the cavity which prevent external air from penetrating.

Schunk et al. (2009) developed a transient heat transfer model of the heat exchanged in an improved version of the ZIRRUS solar reactor. It was employed to predict the thermal behaviour of scaled-up rotary reactors of equivalent design. Taking into account the geometry of the 10 kW reactor, proportional dimensions were considered to scale it up to 100 and 1000 kW. The analysed process was the thermal reduction of ZnO into Zn and O_2. Solar concentration ratio, porosity and extinction coefficient were maintained invariable within the three cases. It was found that the higher the size of the reactor the higher the thermal efficiency. Authors found that thermal efficiency was highly linked to the temperature reached at the reactor walls. Equivalently to what reported about the reactors showed before, the major source of heat losses was re-radiation through the aperture. Also, authors suggested recovering the sensible heat lost with products. ZIRRUS reactor has been scaled up to 100 kW and it has been successfully tested for the ZnO thermal reduction in the solar furnace of Odeillo (France) (Koepf et al., 2015). ZnO dissociation rates as high as 28 g/min were achieved.

Other solar rotary kilns have been reported in literature. At the Plataforma Solar de Almería (PSA), it was constructed a rotary device provided with a quartz window to study the thermal treatment of mercury mine wastes by direct irradiation at temperatures ranging from 200 to 700 °C (Navarro et al., 2014). Experiments to remove Hg minerals from soils and mine wastes were conducted under global radiation of approximately 800 W/m^2 with an exposure time of between 120 and 300 min. The results showed

that lowest values of mercury in treated samples were obtained at a higher temperature and exposition time.

CNRS-PROMES reported the design and construction of a laboratory scale solar rotary kiln. It consisted of a rotary cavity (diameter 0.06 m, length 0.05 m) with a 0.012 m in diameter aperture (Abanades et al., 2007). This small solar reactor was employed for testing the reduction of ZnO into metallic Zn and its design included a feeding system using an Archimedes' screw. The gaseous Zn was condensed and collected in a filter. The reactor worked under reduced pressure what helps the metallic oxides thermal reductions. A hemispherical window was employed to facilitate working with reduced pressure and to keep the window away from the radiation focus. Efforts were realised to determine the best geometry and material of the rotary cavity. They employed cylinders of alumina surrounded by a board of different materials and shapes (Chambon et al., 2010). They searched for avoiding material problems as melting, cracking and for improving the gas stream path. The selected cavity design, finally, was an alumina tube encapsulated in a highly efficient insulation (conductivity of 0.18 W/m K at 1000°C).

Table 1 resumes the main characteristics of solar rotary kiln prototypes. Note that reactor powers and maximum efficiencies could not be directly compared because different authors considered different definitions of them. Maximum temperature refers to particle maximum temperature and the angle of slope was considered positive when the rear part of the reactor was higher than the aperture of the reactor.

Table 1. Summary of the main prototypes of solar rotary kiln reported in literature

Institution	Year	Particle type	Operating mode	Typical mass flow (kg/h) or mass (kg)	Rotating speed (rpm)	Slope (degree)	Maximum Temperature (°C)	Reactor Power (kW)	Reactor Size (m)	Maximum efficiency (%)	Applications	References
PROMES-CNRS	1979	Sand, powder	Continuous	0.036-1.8	4-25	5	1500	2	d 0.02 l 0.09	30	CaO, TES	(Flamant et al., 1980)
DLR	1999	Scraps	Batch	1	0-20	-13	950	10	d 0.2 l 0.4	N.a.	Al	(Funken et al., 1999)
PROMES-CNRS	1999	Granular	Continuous	320, 410, 550	N.a.	5, 8	950	141-160	d 0.64 l 1.2	66	TES	(Sammouda et al., 1999)
PSI	1999	Powder	Continuous	N.a.	N.a.	0	1700	10	d_a 0.06	N.a.	WSTC	(Haueter et al., 1999)
PSI	2003	Granular	Continuous	4	8-18	≠0	1150	10	d 0.252 l 0.225	35	CaO	(Meier et al., 2006)
PSI	2004	Powder	Continuous	0.6-3	2-7	0	1150	10	d 0.6 l 0.35	20	CaO	(Meier et al., 2004)
PSI	2006 (2008)	Powder	Continuous (Semi-batch)	N.a. (0.049, 0.745)	N.a. (30-120)	0	1600 (1900)	10	d_a 0.06 d 0.16 l 0.23	N.a. (1.1-16.9)	WSTC	(Müller et al., 2006), (Shunk et al., 2009)
PROMES-CNRS	2007	Powder	Continuous	0.0036	N.a.	0	2000	N.a.	d_a 0.012 d 0.02 l 0.05	N.a.	WSTC	(Abanades et al., 2007)
DLR	2012	Powder	Batch	0.125, 0.150, 0.250	6	0	900	10	d_a 0.08 d 0.2 l 0.5	N.a.	TCS	(Neises et al., 2012)
PSA	2013	Granular	Batch	N.a.	N.a.	< 0	800	N.a.	N.a.	N.a.	SD	(Navarro et al., 2014)
PSI	2014	Powder	Continuous	0-3.3	N.a.	0	1800	100	d_a 0.52 d 0.58 l 0.83	3	WSTC	(Koepf et al., 2015)
UNAM	2015	Powder	Batch	0.01	4-30	0	1100	10	d 0.067 l 0.074	N.a.	TCS	(Alonso et al., 2015)

N.a. = Not available; (second version);

4.3 Main conclusions and limitations of solar rotary kilns

From the review of the above presented studies, some conclusions connected with the adequacy of performing solar processes in rotary kilns can be inferred:

- If radiation is focused at the kiln aperture, the higher the rate l/d the higher the thermal gradients along the longitudinal axis. A reactor design close to an ideal cavity would help for temperature homogenisation. An aperture of smaller diameter than the reactor drum should be included.
- The rotary kilns show potential to reach high temperatures over 2000 °C.
- Continuous operation mode with controllable residence time makes rotary kilns operationally flexible. It is relevant to count with variable rotational speed to adapt the reactor to the requirements of different processes.
- Attention must be paid to reduce heat losses in rotary kilns. Re-radiation and conduction are two of the identified sources of heat losses. Secondary concentrators can help to decrease the re-radiation losses. If they are used, attention must be paid to maintaining them clear from particles deposition. One found strategy was to separate the drum beginning and the aperture where focusing the radiation by a narrow duct. For prototype optimisation, more than one design-testing step could be required. Insulation improvement or heat recovery including have been are useful for heat losses reducing.
- Good mixing of particles inside the kiln will help the temperature and material homogeneity. It can be achieved with high rotational speed and stirring elements and would improve the process performance. Nevertheless, the most adequate bed motion will depend on the characteristics of the concrete process to carry out.
- Different design strategies can be adopted to improve the process efficiency. Improving the rate of useful radiation (with secondary concentrators) and the capacity of the reactor (giving an inclination degree) would lead to better rates of conversion.
- Instrumentation for temperature measurement is required in order to monitor the process progression. A combination of thermocouples and non-contact measurement systems could help to increase the useful data recording and their quality.
- To control the atmospheres inside the reaction chamber allows extending the field of application of solar rotary kilns. To achieve that, it is useful to incorporate transparent windows, hermetic seals and to work under small overpressure inside the chamber. Window should be maintained cold and clean. This can be achieved by a proper management of the gas streamlines inside the cavity.

Along the previous sections, main aspects of using rotary kilns in solar applications have been reviewed. Limitations of the technology solarisation can be inferred from the findings reported in the reviewed works. They are compiled and discussed below. Design, construction and operation with solar rotary kilns have limitations and most of them are in common with other cavity type solar receivers. On the other hand, computational modelling has been presented as a powerful tool to study the fluid dynamics, the heat and mass transfer phenomena and the chemical reactions that take place in solar rotary kilns. However, some difficulties to simulate the real process usually appear and simplifications and

assumptions are applied in order to obtain approximate solutions. Uncertainties because of the following approximation are usually accepted in literature works.

- For applications of very high temperature, specific materials able to withstand temperature and thermal shock are needed. These materials are not always easy to acquire and they have elevate cost.
- On the contrary of classical rotary kilns, geometrical limitations are associated to solar ones because their performance depends on the radiation-kiln type of contact. For an efficient use of the radiation, it would be helpful to design the reactor as a cavity including an aperture at the front. High d/d_a ratios are convenient in order to decrease re-radiation losses. In tubular solar reactors where the radiation is focused on the front, longer l/d ratios favour a heterogeneous distribution of the radiation along the tube and give rise to higher thermal gradients.
- Accurate temperature measurement in solar rotary kilns is still a significant challenge. The presence of radiation hinders the use of thermocouples inside the rotary bed and non-contact methods involve some restrictions themselves. Thermocouples usually offer reliable measurement but not if they are in direct contact with radiation. Moreover, they may result damaged if radiation impinges on them. On the other hand, non-contact methods need for methodologies to discriminate reflected and emitted radiation and optical properties of the materials must be known.
- In order to allow the radiation to enter, solar rotary kilns should be opened at one of the drum sides. It has been reported operating problems related to leak of material through such an aperture. Some author incorporates a transparent window which, additionally, allows to work under controlled atmospheres. However, attention should be paid to maintaining the window cooled and free of depositions. Otherwise, the window could break by thermal shock and/or reduce its transmittance, with a direct effect on the thermal efficiency of the reactor. Windows may also absorb some radiation wavelength.
- Incoming radiation represents the main contribution to the heat transfer mechanisms in solar reactors. In a solar rotary kiln, radiation impinges on the reactor inner walls but also partially on the other solid parts. To simulate radiation, a flux density profile is usually implemented in the numerical model. While this flux density is usually imposed on the kiln walls, it is often neglected on the other parts. Otherwise, the computational cost would be much higher.
- Optical properties of materials considered in models should be correctly imposed to achieve accurate solutions. The absorption and emission of solar radiation at the receiver surfaces are defined by complex functions for wavelength and direction which rarely are available. Simplifications have been found which considered grey, diffuse and opaque kiln walls with radiative properties independent of the temperature.
- Some simulation models, as the S2S, are usually employed to reduce calculation time although they are not able to deliver accurate results. For example, S2S model does not consider semi-transparent medium as windows, neither particles suspension nor high temperature gaseous medium. Thus, its use is limited to approximate calculation or in combination with other models.

5. Conclusions

The present work overviews the use of rotary kilns in industrial high temperature applications and those aspects related to their adaptation to CSP technologies. Main characteristics which define rotary kilns performance are the type of bed motion, given by the Fr number, and the residence time. Rotary kilns devices have been selected as solar receivers or reactors in several examples, and the main reason is they are well-known and extensively proved systems in classical industry. However, in this review, significant differences between classical and solar rotary kilns have been identified.

Different numerical and experimental works on solar rotary kilns have been reviewed and the main conclusions obtained in each one have been discussed along this work. Authors have faced the difficulties to model radiative transfer by the use of different assumptions. They depend on the thermochemical process accomplished, the computational cost and the desired accuracy. From experimental studies revision, it can be concluded that several successful results have been obtained on the performing of thermal and thermochemical solar processes. However, in most of the cases, the initial prototypes did not given rise to high efficiencies and authors applied different strategies for improving them, denoting the grade of complexity of the reactor design stage. A novel solar reactor, which initially was able to operate as a rotary kiln and a packed bed, allowed for experimentally proving the advantages of the rotary operation mode concerning the good mixing of particles and homogeneous distribution of temperature in the reaction chamber.

Further investigations on solar rotary kilns should aim to extent the application field to those typical of classical industry. Metallurgy of certain metals, such as lead, cupper, or iron could be among the most promising examples. These novel applications should be investigated for industrial scale solar rotary kilns that could be integrated in a central tower solar plant.

Some recommendation for further investigations can be deduced from the conclusions of this work. Optimising solar rotary kilns designs is still an essential challenge. Available knowledge on classical industry rotary kilns should be considered in order to improve the solar rotary kilns technology and processes efficiency. Operational conditions of classical rotary kilns are usually carefully selected in order to obtain as much parameters uniformity as possible in the particles bed. Rolling mode has been identified as advantageous for this purpose. In the solar field, reviewed works do not pay particular attention to the motion mode analysis and definition. An additional effort in such a direction could worth it because better uniformity conditions could give rise to better efficiency results. A deep analysis of parameters such as main dimensions, slope, fill ratio, rotation speed, etc., as well as particles characteristics, would help in the design stage. Furthermore, the introduction of internal elements as paddles, fins or lifters in the drum has not been considered in solar prototypes so far, while it is a typical improvement of the classical rotary kilns. Main differences between classical and solar rotary kilns are related to the heat transfer mechanisms that dominate the heat interchange. Convection between hot gas and solid material is often the main mechanism in classical rotary kilns, although a good agreement among works has not been found in this sense because there may be a strong dependence on the

working temperature and the reactor design. In the case of solar devices, radiation represents always the main contribution to heat transfer in the kiln and re-radiation through the aperture the main source of heat losses. In fact, solar rotary kilns are a particular type of cavity receivers. Due to it, many of their features and limitations are common to other cavity receivers.

In summary, rotary kilns appear to be suitable devices to perform solar advanced applications of high temperature. Future investigations should be aimed to extent the number of process carried out in solar rotary kilns and to improve and scale up the receivers/reactors on the basis of the classical industrial knowledge.

Acknowledgements

The authors acknowledge the financial support provided by the FONDECYT project number 3150026 of CONICYT (Chile), the Education Ministry of Chile Grant PMI ANT 1201, as well as CONICYT/ FONDAP/ 15110019 "Solar Energy Research Center" SERC-Chile. Also, the second author wish to thank to the Plataforma Solar de Almería and the University of Almería for the collaboration and assistance devoted to the development of his Ph.D research.

References

Abanades, S., Charvin, P., Flamant, G., 2007. Design and simulation of a solar chemical reactor for the thermal reduction of metal oxides: Case study of zinc oxide dissociation. Chem. Eng. Sci. 62, 6323–6333. doi:10.1016/j.ces.2007.07.042

Abanades, S., Charvin, P., Flamant, G., Neveu, P., 2006. Screening of water-splitting thermochemical cycles potentially attractive for hydrogen production by concentrated solar energy. Energy 31, 2805–2822. doi:10.1016/j.energy.2005.11.002

Agrafiotis, C., Roeb, M., Sattler, C., 2015. A review on solar thermal syngas production via redox pair-based water/carbon dioxide splitting thermochemical cycles. Renew. Sustain. Energy Rev. 42, 254–285. doi:10.1016/j.rser.2014.09.039

Agrafiotis, C., Roeb, M., Schmücker, M., Sattler, C., 2014. Exploitation of thermochemical cycles based on solid oxide redox systems for thermochemical storage of solar heat. Part 1: Testing of cobalt oxide-based powders. Sol. Energy 102, 189–211. doi:10.1016/j.solener.2013.12.032

Alexopoulos, S.O., Dersch, J., Roeb, M., Pitz-Paal, R., 2015. Simulation model for the transient process behaviour of solar aluminium recycling in a rotary kiln. Appl. Therm. Eng. 78, 387–396. doi:10.1016/j.applthermaleng.2015.01.007

Alonso, E., Hutter, C., Romero, M., Steinfeld, A., Gonzalez-aguilar, J., 2013. Kinetics of $Mn_2O_3 - Mn_3O_4$ and $Mn_3O_4 - MnO$ redox reactions performed under concentrated thermal radiative flux.

Alonso, E., Pérez-Rábago, C., Licurgo, J., Fuentealba, E., Estrada, C.A., 2015. First experimental studies of solar redox reactions of copper oxides for thermochemical energy storage. Sol. Energy 115, 297–305. doi:10.1016/j.solener.2015.03.005

Alonso, E., Romero, M., 2015a. Review of experimental investigation on directly irradiated particles solar reactors. Renew. Sustain. Energy Rev. 41, 53–67. doi:10.1016/j.rser.2014.08.027

Alonso, E., Romero, M., 2015b. A directly irradiated solar reactor for kinetic analysis of non-volatile metal oxides reductions. Int. J. Energy Res. doi:10.1002/er

Bianchini, A., Pellegrini, M., Saccani, C., 2015. Solar steam reforming of natural gas integrated with a gas

turbine power plant: Economic assessment. Sol. Energy 122, 1342–1353. doi:10.1016/j.solener.2015.10.046

Boateng, A.A., 2008. The rotary kiln evolution and phenomenon, in: Rotary kilns. Elsevier Inc., pp. 1–14. doi:10.1016/B978-075067877-3.50003-9

Boateng, A.A., Barr, P.V., 1996. A thermal model for the rotary kiln including heat transfer within the bed. Int. J. Heat Mass Transf. 39, 2131–2147. doi:10.1016/0017-9310(95)00272-3

Boateng, A.A., Barr, P. V., 1996. Modelling of particle mixing and segregation in the transverse plane of a rotary kiln. Chem. Eng. Sci. 51, 4167–4181. doi:10.1016/0009-2509(96)00250-3

Brimacombe, J.K., Watkinson, A.P., 1978. Heat transfer in a direct-fired rotary kiln: I. Pilot plant and experimentation. Metall. Trans. B 9, 201–208. doi:10.1007/BF02653685

Carvalho, M.G., Farias, T., Martius, A., 1995. A three-dimensional modelling of the radiative heat transfer in a cement kiln, in: Combustion technologies for a clean environment. p. 146.

Chambon, M., Abanades, S., Flamant, G., 2010. Design of a lab-cale rotary cavity-type solar reactor for continuous thermal dissociation of volatile oxides under reduced pressure. J. Sol. Energy Eng. 132, 21006. doi:10.1115/1.4001147

Cholette, A., Cloutier, L., 1959. Mixing efficiency determinations for continuous flow systems. Can. J. Chem. Eng. 37, 105–112. doi:10.1002/cjce.5450370305

Chueh, W.C., Falter, C., Abbott, M., Scipio, D., Furler, P., Haile, S.M., Steinfeld, A., 2010. High-flux solar-driven thremochemical dissociation of CO_2 and H_2O using nonstoichiometric ceria. Science, 330, 1797–1801. doi:10.1126/science.1197834.

Descoins, N., Dirion, J.-L., Howes, T., 2005. Solid transport in a pyrolysis pilot-scale rotary kiln: preliminary results—stationary and dynamic results. Chem. Eng. Process. Process Intensif. 44, 315–321. doi:10.1016/j.cep.2004.02.025

Dhanjal, S.K., Barr, P. V., Watkinson, a. P., 2004. The rotary kiln: An investigation of bed heat transfer in the transverse plane. Metall. Mater. Trans. B 35, 1059–1070. doi:10.1007/s11663-004-0062-0

Diver, R.B., Miller, J.E., Allendorf, M.D., Siegel, N.P., Hogan, R.E., 2008. Solar Thermochemical Water-Splitting Ferrite-Cycle Heat Engines. J. Sol. Energy Eng. 130, 41001. doi:10.1115/1.2969781

Duchesne, C., Thibault, J., Bazin, C., 1996. Modeling of the Solids Transportation within an Industrial Rotary Dryer: A Simple Model. Ind. Eng. Chem. Res. 35, 2334–2341. doi:10.1021/ie950625j

Flamant, G., 1980. Thermochimie solaire à hautes températures, résultats expérimentaux. Quelques perspectives d'application. Rev. Phys. Appliquée 15, 503–511.

Flamant, G., Hernandez, D., Bonet, C., Traverse, J.-P., 1980. Experimental aspects of the thermochemical conversion of solar energy; Decarbonation of $CaCO_3$. Sol. Energy 24, 385–395. doi:10.1016/0038-092X(80)90301-1

Francis, T.M., Lichty, P.R., Weimer, A.W., 2010. Manganese oxide dissociation kinetics for the Mn_2O_3 thermochemical water-splitting cycle. Part 1: Experimental. Chem. Eng. Sci. 65, 3709–3717. doi:10.1016/j.ces.2010.03.002

Fresno, F., Fernández-Saavedra, R., Belén Gómez-Mancebo, M., Vidal, A., Sánchez, M., Isabel Rucandio, M., Quejido, A.J., Romero, M., 2009. Solar hydrogen production by two-step thermochemical cycles: Evaluation of the activity of commercial ferrites. Int. J. Hydrogen Energy 34, 2918–2924. doi:10.1016/j.ijhydene.2009.02.020

Funken, K.H., Pohlmann, B., Lüpfert, E., Dominik, R., 1999. Application of concentrated solar radiation to high temperature detoxification and recycling processes of hazardous wastes. Sol. Energy 65, 25–31. doi:10.1016/S0038-092X(98)00089-9

Fuqiang, W., Jianyu, T., Huijian, J., Yu, L., 2015. Thermochemical performance analysis of solar driven CO_2 methane reforming. Energy 91, 645–654. doi:10.1016/j.energy.2015.08.080

Gallo, A., Roldán, M.I., Alonso, E., Fuentealba, E., 2016. Considerations for using a rotary kiln for high temperature industrial processes with and without thermal storage, in: 11 ISES EuroSun Conference. Palma de Mallorca (Spain).

Glasmacher-Remberg, C., Roeb, M., Dersch, J., Schäfer, R., Funken, K.-, H., 2001. Solar thermal recycling of aluminium. AL Alum. Its Alloy. 135, 73–77.

Gokon, N., Takahashi, S., Yamamoto, H., Kodama, T., 2008. Thermochemical two-step water-splitting reactor with internally circulating fluidized bed for thermal reduction of ferrite particles. Int. J. Hydrogen Energy 33, 2189–2199. doi:10.1016/j.ijhydene.2008.02.044

Gorog, J.P., Adams, T.N., Brimacombe, J.K., 1983. Heat transfer from flames in a rotary kiln. Metall. Trans. B 14, 411–424. doi:10.1007/BF02654360

Halmann, M., Frei, A., Steinfeld, A., 2007. Carbothermal reduction of alumina: Thermochemical equilibrium calculations and experimental investigation. Energy 32, 2420–2427. doi:10.1016/j.energy.2007.06.002

Harper-International, 2016. Rotary tube furnaces. Company webpage: URL http://www.harperintl.com/technologies/high-temp-furnaces/rotary-furnaces/ (accessed 12.28.16).

Haueter, P., Moeller, S., Palumbo, R., Steinfeld, a, 1999. The production of zinc by thermal dissociation of zinc oxide - Solar chemical reactor design. Sol. Energy 67, 161–167. doi:10.1016/S0038-092x(00)00037-2

Henein, H., Brimacombe, J.K., Watkinson, A.P., 1983. Experimental study of transverse bed motion in rotary kilns. Metall. Trans. B 14, 191–205. doi:10.1007/BF02661016

Iguaz, A., Esnoz, A., Martínez, G., López, A., Vírseda, P., 2003. Mathematical modelling and simulation for the drying process of vegetable wholesale by-products in a rotary dryer. J. Food Eng. 59, 151–160. doi:10.1016/S0260-8774(02)00451-X

Kaleemullah, S., Kailappan, R., 2005. Drying Kinetics of Red Chillies in a Rotary Dryer. Biosyst. Eng. 92, 15–23. doi:10.1016/j.biosystemseng.2005.05.015

Kaneko, H., Miura, T., Fuse, A., Ishihara, H., Taku, S., Fukuzumi, H., Naganuma, Y., Tamaura, Y., 2007. Rotary-type solar reactor for solar hydrogen production with two-step water splitting process. Energy and Fuels 21, 2287–2293. doi:10.1021/ef060581z

Kim, K., Siegel, N., Kolb, G., Rangaswamy, V., Moujaes, S.F., 2009. A study of solid particle flow characterization in solar particle receiver. Sol. Energy 83, 1784–1793. doi:10.1016/j.solener.2009.06.011

Koepf, E., Villasmil, W., Meier, A., 2015. Pilot-scale solar reactor operation and characterization for fuel production via the Zn/ZnO thermochemical cycle. Appl. Energy 165, 1004–1023. doi:10.1016/j.apenergy.2015.12.106

Li, A.M., Li, X.D., Li, S.Q., Ren, Y., Shang, N., Chi, Y., Yan, J.H., Cen, K.F., 1999. Experimental studies on municipal solid waste pyrolysis in a laboratory-scale rotary kiln. Energy 24, 209–218. doi:10.1016/S0360-5442(98)00095-4

Ludwig, C.B., Malkmus, W., Reardon, J.E., Thomson, J.A.L., 1973. Handbook of infrared radiation from combustion gases. NASA Spec. NASA SP-30.

Maag, G., Zanganeh, G., Steinfeld, A., 2009. Solar thermal cracking of methane in a particle-flow reactor for the co-production of hydrogen and carbon. Int. J. Hydrogen Energy 34, 7676–7685. doi:10.1016/j.ijhydene.2009.07.037

Mastorakos, E., Massias, A., Tsakiroglou, C.D., Goussis, D. A., Burganos, V.N., Payatakes, A. C., 1999. CFD predictions for cement kilns including flame modelling, heat transfer and clinker chemistry. Appl. Math. Model. 23, 55–76. doi:10.1016/S0307-904X(98)10053-7

Meier, A., Bonaldi, E., Cella, G.M., Lipinski, W., 2005a. Multitube rotary kiln for the industrial solar production of lime. J. Sol. Energy Eng. 127, 386–395. doi:10.1115/1.1979517

Meier, A., Bonaldi, E., Cella, G.M., Lipinski, W., Wuillemin, D., 2006. Solar chemical reactor technology for industrial production of lime. Sol. Energy 80, 1355–1362. doi:10.1016/j.solener.2005.05.017

Meier, A., Bonaldi, E., Cella, G.M., Lipinski, W., Wuillemin, D., Palumbo, R., 2004. Design and experimental investigation of a horizontal rotary reactor for the solar thermal production of lime. Energy 29, 811–821. doi:10.1016/S0360-5442(03)00187-7

Meier, A., Gremaud, N., Steinfeld, A., 2005b. Economic evaluation of the industrial solar production of lime. Energy Convers. Manag. 46, 905–926. doi:10.1016/j.enconman.2004.06.005

Mellmann, J., 2001. The transverse motion of solids in rotating cylinders-forms of motion and transition behavior. Powder Technol. 118, 251–270. doi:10.1016/S0032-5910(00)00402-2

Moller, S., Palumbo, R., 2001. Solar thermal decomposition kinetics of ZnO in the temperature range 1950 – 2400 K. Chem. Eng. Sci. 56, 4505–4515. doi: 10.1016/S0009-2509(01)00113-0

Müller, R., Haeberling, P., Palumbo, R.D., 2006. Further advances toward the development of a direct heating solar thermal chemical reactor for the thermal dissociation of ZnO(s). Sol. Energy 80, 500–511. doi:10.1016/j.solener.2005.04.015

Müller, R., Lipinski, W., Steinfeld, A., 2008. Transient heat transfer in a directly-irradiated solar chemical reactor for the thermal dissociation of ZnO. Appl. Therm. Eng. 28, 524–531. doi:10.1016/j.applthermaleng.2007.05.002

Navarro, A., Canadas, I., Rodriguez, J., 2014. Thermal Treatment of Mercury Mine Wastes Using a Rotary Solar Kiln. Minerals 4, 37–51. doi:10.3390/min4010037

Neises, M., Tescari, S., de Oliveira, L., Roeb, M., Sattler, C., Wong, B., 2012. Solar-heated rotary kiln for thermochemical energy storage. Sol. Energy 86, 3040–3048. doi:10.1016/j.solener.2012.07.012

Nikulshina, V., Gebald, C., Steinfeld, A., 2009. CO_2 capture from atmospheric air via consecutive CaO-carbonation and $CaCO_3$-calcination cycles in a fluidized-bed solar reactor. Chem. Eng. J. 146, 244–248. doi:10.1016/j.cej.2008.06.005

Orfila, M., Linares, M., Molina, R., Botas, J.Á., Sanz, R., Marugán, J., 2016. Perovskite materials for hydrogen production by thermochemical water splitting. Int. J. Hydrogen Energy 41, 19329–19338. doi:10.1016/j.ijhydene.2016.07.041

Palmer, G., Howes, T., 1998. Heat Transfer in Rotary Kilns. Cem. Ind. Fed. Tech. Conf. 1–6. doi:10.1007/BF02664572

Palumbo, R., Keunecke, M., M??ller, S., Steinfeld, A., 2004. Reflections on the design of solar thermal chemical reactors: Thoughts in transformation. Energy 29, 727–744. doi:10.1016/S0360-5442(03)00180-4

Pardo, P., Deydier, A., Anxionnaz-Minvielle, Z., Rougé, S., Cabassud, M., Cognet, P., 2014. A review on high temperature thermochemical heat energy storage. Renew. Sustain. Energy Rev. 32, 591–610. doi:10.1016/j.rser.2013.12.014

Piatkowski, N., Wieckert, C., Steinfeld, A., 2009. Experimental investigation of a packed-bed solar reactor for the steam-gasification of carbonaceous feedstocks. Fuel Process. Technol. 90, 360–366. doi:10.1016/j.fuproc.2008.10.007

Puig-Arnavat, M., Tora, E. a., Bruno, J.C., Coronas, a., 2013. State of the art on reactor designs for solar gasification of carbonaceous feedstock. Sol. Energy 97, 67–84. doi:10.1016/j.solener.2013.08.001

Renaud, M., Thibault, J., Trusiak, A., 2000. Solids Transportation Model of an Industrial Rotary Dryer. Dry. Technol. 18, 843–865. doi:10.1080/07373930008917741

Roeb, M., Säck, J.-P., Rietbrock, P., Prahl, C., Schreiber, H., Neises, M., de Oliveira, L., Graf, D., Ebert, M., Reinalter, W., Meyer-Grünefeldt, M., Sattler, C., Lopez, A., Vidal, A., Elsberg, A., Stobbe, P., Jones, D., Steele, A., Lorentzou, S., Pagkoura, C., Zygogianni, A., Agrafiotis, C., Konstandopoulos, A. G., 2011. Test operation of a 100kW pilot plant for solar hydrogen production from water on a solar

tower. Sol. Energy 85, 634–644. doi:10.1016/j.solener.2010.04.014
Sai, P.S.T., Surender, G.D., Damodaran, A.D., Suresh, V., Philip, Z.G., Sankaran, K., 1990. Residence time distribution and material flow studies in a rotary kiln. Metall. Mater. 21, 1005–1011. doi:10.1007/BF02670271
Sammouda, H., Royere, C., Belghith, A., Maalej, M., 1999. Heat transfer in a rotating furnace of a solar sand-boiler at a 1000 kW thermal concentration system. Renew. Energy 17, 21–47. doi:10.1016/S0960-1481(98)00037-8
Schunk, L.O., Haeberling, P., Wepf, S., Wuillemin, D., Meier, A., Steinfeld, A., 2008. A Receiver-Reactor for the Solar Thermal Dissociation of Zinc Oxide. J. Sol. Energy Eng. 130, 21009. doi:10.1115/1.2840576
Schunk, L.O., Lipiński, W., Steinfeld, A., 2009. Heat transfer model of a solar receiver-reactor for the thermal dissociation of ZnO - Experimental validation at 10 kW and scale-up to 1 MW. Chem. Eng. J. 150, 502–508. doi:10.1016/j.cej.2009.03.012
Schunk, L.O., Steinfeld, A., 2009. Kinetics of the Thermal Dissociation of ZnO Exposed to Concentrated Solar Irradiation Using a Solar-Driven Thermogravimeter in the 1800 – 2100 K Range. AIChE J. 2, 1497–1504. doi:10.1002/aic
Shahin, H., Hassanpour, S., Saboonchi, A., 2016. Thermal energy analysis of a lime production process: Rotary kiln, preheater and cooler. Energy Convers. Manag. 114, 110–121. doi:10.1016/j.enconman.2016.02.017
Steinfeld, A., Frei, A., Kuhn, P., Wuillemin, D., 1995. Solar thermal production of zinc and syngas via combined ZnO-reduction and CH4-reforming processes. Int. J. Hydrogen Energy 20, 793–804. doi:10.1016/0360-3199(95)00016-7
Tan, T., Chen, Y., 2010. Review of study on solid particle solar receivers. Renew. Sustain. Energy Rev. 14, 265–276. doi:10.1016/j.rser.2009.05.012
Tescari, S., Neises, M., de Oliveira, L., Roeb, M., Sattler, C., Neveu, P., 2013. Thermal model for the optimization of a solar rotary kiln to be used as high temperature thermochemical reactor. Sol. Energy 95, 279–289. doi:10.1016/j.solener.2013.06.021
Trombe, F., 1973. First results obtained with the 100kW solar furnace. Sol. Energy 15, 63–66. doi:10.1016/0038-092x(73)90007-8
Trombe, F., 1963. Solar furnaces for high-temperature processing. Sol. Energy 7, 100–107. doi:10.1016/0038-092X(63)90035-5
Trombe, F., Foex, M., 1954. Utilisation de fours centrifuges pour le traitement par l'énergie solaire des substances à haute température. Bull. Soc. Chim. Fr. 1315–1322.
Tscheng, S.H., Watkinson, A.P., 1979. Convective heat transfer in a rotary kiln. Can. J. Chem. Eng. 57, 433–443. doi:10.1002/cjce.5450570405
Vijayan, S.N., Sendhilkumar, S., 2014. Industrial applications of rotary kiln in various sectors - A Review. Int. J. Eng. Innov. Res. 3, 342–345.
Watkinson, A.P., Brimacombe, J.K., 1978. Heat transfer in a direct-fired rotary kiln: II. Heat flow results and their interpretation. Metall. Trans. B 9, 209–219. doi:10.1007/BF02653686
Wey, M.-Y., Liu, K.-Y., Tsai, T.-H., Chou, J.-T., 2006. Thermal treatment of the fly ash from municipal solid waste incinerator with rotary kiln. J. Hazard. Mater. 137, 981–9. doi:10.1016/j.jhazmat.2006.03.024
Wieckert, C., Palumbo, R., Frommherz, U., 2004. A two-cavity reactor for solar chemical processes: Heat transfer model and application to carbothermic reduction of ZnO. Energy 29, 771–787. doi:10.1016/S0360-5442(03)00183-X
Yang, L., Farouk, B., 1997. Modeling of solid particle flow and heat transfer in rotary kiln calciners. J. Air Waste Manage. Assoc. 47, 1189–1196. doi:10.1080/10473289.1997.10464069
Yang, Y., Rakhorst, J., Reuter, M., Jhl, 1999. Analysis of gas flow and mixing in a rotary kiln waste incinerator. Second Int. Conf. CFD Miner. Process Ind. 443–448.

Zhang, Y.J., Barr, P. V., Meadowcroft, T.R., 2008. Scrap melting in continuous process rotary melting furnace part 1 – bench scale furnace trials. Ironmak. Steelmak. 35, 600–609. doi:10.1179/174328107X255023

Zhou, B., Yang, Y., Reuter, M.A., Boin, U.M.J., 2006. Modelling of aluminium scrap melting in a rotary furnace. Miner. Eng. 19, 299–308. doi:10.1016/j.mineng.2005.07.017